

# Alternative expression for the maximum potential intensity of tropical cyclones

Anastassia M. Makarieva<sup>1</sup> and Andrei V. Nefiodov<sup>1</sup>

<sup>1</sup>Theoretical Physics Division, Petersburg Nuclear Physics Institute, Gatchina 188300, St. Petersburg, Russia

*Correspondence to:* A. M. Makarieva (ammakarieva@gmail.com)

**Abstract.** Emanuel’s Maximum Potential Intensity (E-PI) derives the maximum velocity of tropical cyclones from environmental parameters based on distinct sets of assumptions applied to the upper atmosphere, the boundary layer and the air-sea interface. At the top of the boundary layer at the radius of maximum wind E-PI relates the centrifugal acceleration (squared maximum velocity divided by radius) to the radial gradient of saturated moist entropy. The proportionality coefficient equals the difference between air temperatures in the outflow region and at the top of the boundary layer. We show that a different relationship between the same quantities derives straightforwardly from the definition of saturated moist entropy and the gradient wind balance. Here the proportionality coefficient depends on the local mixing ratio of water vapor and the degree of adiabaticity of the radial gradient of air temperature. The robust alternative relationship reveals that when, as originally assumed in the E-PI derivation, the air is horizontally isothermal, E-PI at the top of the boundary layer underestimates the squared maximum velocity by approximately twofold. This provides an explanation to the “superintensity” phenomenon (maximum wind speeds exceeding E-PI). The discrepancy increases (diminishes) when the air temperature at the point of maximum wind declines (grows) towards the storm center. The established theoretical relationships are illustrated with the data for Hurricane Isabel 2003 and their implications for assessing the maximum intensity of tropical storms are discussed.

## 1 Introduction

Tropical storms threaten human lives and livelihoods. Numerical models can simulate a wide range of storm intensities under the same environmental conditions (e.g., Tao et al., 2020). Thus it is desirable to have a reliable theoretical framework that would, from the first principles, confine model outputs to the reality domain (Emanuel, 2020). The theoretical formulation for maximum potential intensity of tropical cyclones by Emanuel (1986) (E-PI) has been long considered as a robust upper limit on storm intensity (see discussions by Garner (2015), Kieu and Moon (2016) and Kowaleski and Evans (2016)). At the same time, the phenomenon of “superintensity”, when the observed or modelled storm velocities exceed E-PI, has been perceived as an important research challenge (e.g., Persing and Montgomery, 2003; Montgomery et al., 2006; Bryan and Rotunno, 2009; Rousseau-Rizzi and Emanuel, 2019; Li et al., 2020). Since the strongest storms are the most dangerous ones, it is important to understand when and why the theoretical limits can be exceeded. The principal way of approaching the superintensity problem was to reveal how the E-PI assumptions can be modified to yield greater intensities. For example, Montgomery et al. (2006) suggested that superintensity could result from an additional heat source provided by the storm eye (a source of energy not

considered in E-PI). Bryan and Rotunno (2009) investigated how superintensity could result from the flow being supergradient (while E-PI assumed the gradient wind balance). For a recent overview of superintensity assessments in modelling studies see Rousseau-Rizzi and Emanuel (2019).

Here we present a different approach. We show that, even in the case when all the E-PI assumptions hold, E-PI will systematically underestimate storm intensities provided the air is horizontally isothermal at the point of maximum wind. Horizontal isothermy of the top of the boundary layer was assumed by Emanuel (1986) in his original derivation of E-PI. As we will discuss, it is indeed a physically plausible assumption.

That under horizontal isothermy E-PI underestimates storm intensity, follows straightforwardly from the definition of saturated moist entropy. At the point of maximum wind E-PI relates the radial gradients  $\partial s^*/\partial r$  and  $\partial p/\partial r$  of saturated moist entropy  $s^*$  and air pressure  $p$  via an external parameter (the outflow temperature  $T_o$ ). However,  $s^*$  being a state variable, its radial gradient is a local function of the radial gradients of air pressure  $p$  and temperature  $T$ . Thus, specifying a relationship between  $\partial s^*/\partial r$  and  $\partial p/\partial r$  uniquely sets  $\partial T/\partial r$ . Conversely, setting  $\partial T/\partial r = 0$  relates  $\partial s^*/\partial r$  and  $\partial p/\partial r$  in a specific way that, under common atmospheric conditions, is shown here to be incompatible with E-PI.

We derive the alternative relationship between the radial gradient of saturated moist entropy and maximum velocity in Section 2, illustrate the obtained relationships with the data for Hurricane Isabel 2003 in Section 3 and discuss their implications for assessing the intensity limits of tropical storms in Section 4.

## 2 Different expressions for maximum intensity

### 2.1 Conventional E-PI

E-PI has three blocks, with distinct set of assumptions applied to each block: the upper atmosphere including the top of the boundary layer, the interior of the boundary layer and the ocean-atmosphere interface. Here we focus on the first block.

For the upper atmosphere, the key relationship of E-PI is between saturated moist entropy  $s^*$  and angular momentum  $M$  (for a compact derivation see Emanuel and Rotunno, 2011, Eq. 13):

$$-(T - T_o) \frac{ds^*}{dM} = \frac{v}{r} + \frac{f}{2}, \quad z \geq z_b, \quad (1)$$

where

$$M = vr + \frac{1}{2}fr^2, \quad (2)$$

$z_b$  is the height of the boundary layer,  $r$  is the distance from the storm center,  $T$  is the local air temperature,  $T_o$  corresponds to  $r \rightarrow \infty$  on a streamline defined by a given value of  $ds^*/dM$ ,  $v$  is the tangential velocity. The Coriolis parameter  $f \equiv 2\Omega \sin \varphi$  is assumed constant ( $\varphi$  is latitude,  $\Omega$  is the angular velocity of Earth's rotation). For the definition of saturated moist entropy see Eq. (A.2) in the Appendix.

Relationship (1) derives from the assumptions of hydrostatic and gradient wind balance and from the statement that surfaces of constant  $s^*$  and  $M$  coincide (Emanuel, 1986; Emanuel and Rotunno, 2011). Using the definition of angular momentum (2),

Eq. (1) can be re-written as follows (see Emanuel, 1986, Eq. 13):

$$(T - T_o) \frac{\partial s^*}{\partial r} = -\frac{M}{r^2} \frac{\partial M}{\partial r}. \quad (3)$$

At the point  $(r_m, z_m)$  of maximum wind, provided that  $f \ll v_m/r_m$  and  $\partial v/\partial r \ll v_m/r_m$ , Eq. (3) becomes (see, e.g., Bell and Montgomery, 2008, their Eq. 5 and our Eq. (A.1) in the Appendix):

$$\varepsilon T_b \frac{\partial s^*}{\partial r} = -\frac{v_m^2}{r_m}, \quad (4)$$

where  $\varepsilon \equiv (T_b - T_o)/T_b$  is the Carnot efficiency. E-PI assumes that the point of maximum wind is located at the top of the boundary layer, i.e.  $T = T_b$  at  $(r_m, z_m)$ , where  $z_m = z_b$  (Emanuel, 1986; Emanuel and Rotunno, 2011).

In gradient wind balance,

$$\alpha \frac{\partial p}{\partial r} = \frac{v^2}{r} + fv, \quad (5)$$

where  $p$  is air pressure and  $\alpha \equiv 1/\rho$  is inverse air density, Eq. (4), with  $fv$  neglected, becomes

$$\varepsilon T_b \frac{\partial s^*}{\partial r} = -\alpha \frac{\partial p}{\partial r}. \quad (6)$$

We recapitulate that Eq. (6) is valid at the point of maximum wind under the same assumptions as does Eq. (1).

## 2.2 An alternative expression for maximum intensity

Since saturated moist entropy  $s^*$  is a state variable, its radial gradient can be expressed in terms of the radial gradients of air pressure and temperature (see Eq. (A.9) in the Appendix):

$$\frac{1}{1 + \zeta} T \frac{\partial s^*}{\partial r} = -\alpha_d \frac{\partial p}{\partial r} \left( 1 - \frac{1}{\Gamma} \frac{\partial T/\partial r}{\partial p/\partial r} \right), \quad (7)$$

where  $\zeta \equiv L\gamma_d^*/(RT)$ ,  $R = 8.3 \text{ J mol}^{-1} \text{ K}^{-1}$  is the universal gas constant,  $\gamma_d^* \equiv p_v^*/p_d$ ,  $p_v^*$  is the saturated water vapor pressure,  $p_d$  is the partial pressure of dry air,  $L \approx 45 \text{ kJ mol}^{-1}$  is the latent heat of vaporization,  $\Gamma$  ( $\text{K Pa}^{-1}$ ) is the moist adiabatic lapse rate of air temperature (see its definition (A.10) in the Appendix),  $\alpha_d \equiv 1/\rho_d$  is the inverse dry air density.

Equation (7) does not contain any assumptions but follows directly from the definition of saturated moist entropy. Being generally valid, Eq. (7) can be used to examine the validity of E-PI's Eq. (6). For simplicity, taking into account that  $q^* \sim 10^{-2} \ll 1$ , we assume in Eq. (7)  $\alpha_d = (1 + q^*)\alpha \approx \alpha$ .

## 3 Comparison of E-PI at the top of boundary layer, Eq. (6), with Eq. (7)

### 3.1 Horizontal isothermy

Referring to observations and to Frank (1977), Emanuel (1986, p. 588) in his original derivation of E-PI assumed the top of the boundary layer to be isothermal. With  $\partial T/\partial r = 0$ , the expression in braces in the right-hand side of Eq. (7),

$$C \equiv 1 - \frac{1}{\Gamma} \frac{\partial T/\partial r}{\partial p/\partial r}, \quad (8)$$

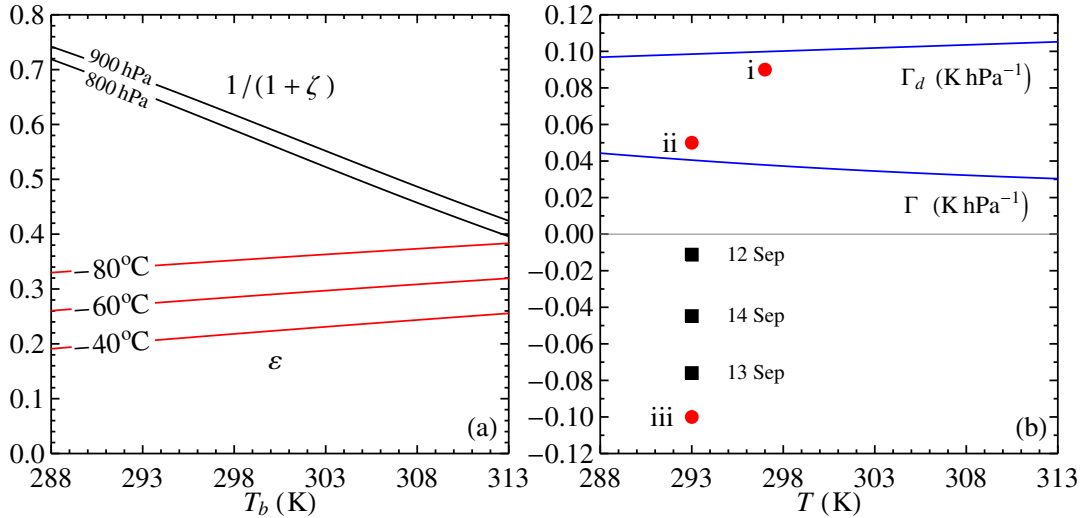


**Figure 1.** Parameters  $\varepsilon$  versus  $1/(1+\zeta)$  (a) and moist  $\Gamma$  and dry  $\Gamma_d$  adiabatic temperature gradients (b) as dependent on temperature. The  $\varepsilon \equiv (T_b - T_o)/T_b$  curves correspond to different outflow temperatures  $T_o$ ; the  $1/(1+\zeta)$  curves correspond to  $p_d$  values of 800 and 900 hPa, see Eq. (A.10);  $\Gamma$  and  $\Gamma_d$  are calculated for  $p = 850$  hPa. In (b), the circles indicate the *mean* temperature gradients (K hPa<sup>-1</sup>) observed in Hurricane Isabel 2003 on September 13 between the eyewall and the outer core at the surface (i) and at the top of the boundary layer (ii) and between the eye and the eyewall at the top of the boundary layer (iii); the squares indicate the *local* temperature gradients (K hPa<sup>-1</sup>) at the point of maximum wind calculated from Eq. (11) and the data of Table 1 for Hurricane Isabel 2003 on 12, 13 and 14 September. See Section 3.2 for calculation details.

equals unity. In this case E-PI's Eq. (6) can only be valid if

$$\varepsilon = \frac{1}{1+\zeta}. \quad (9)$$

In the terrestrial atmosphere such conditions appear to be rare (Fig. 1a). The maximum Carnot efficiency estimated from the temperatures observed in the outflow and at the top of the boundary layer is  $\varepsilon = 0.35$  (DeMaria and Kaplan, 1994). The minimum value of  $1/(1+\zeta) = 0.5$  is 1.4-fold larger. It corresponds to the largest  $\gamma_d^* \approx 0.05$  for  $T_b = 303$  K (30°C) and  $p_d \approx p = 800$  hPa.

The partial pressure  $p_v^*$  of saturated water vapor and, hence,  $\gamma_d^*$  depend exponentially on air temperature. The realistic temperatures at the top of the boundary layer are commonly significantly lower than 303 K. Thus, the discrepancy between E-PI and Eq. (7) should be commonly significantly higher (Fig. 1a).

In the general case, instead of the gradient wind balance (5), we can write

$$\alpha \frac{\partial p}{\partial r} \equiv \mathcal{B} \frac{v^2}{r}, \quad (10)$$

where  $\mathcal{B}$  defines the degree to which the flow is radially unbalanced:  $\mathcal{B} < 1$  for the supergradient flow when the outward-directed centrifugal force is larger than the inward-pulling pressure gradient. For example, in Hurricane Isabel 2003 on September 13 the tangential wind was estimated at the top of the boundary layer as being 15% supergradient (Bell and Montgomery,

2008). This corresponds to  $\mathcal{B} = 1/(1.15)^2 \approx 0.8$ . For the supergradient wind in the numerical experiment of Bryan and Rotunno (2009, Fig. 8),  $\mathcal{B} \approx 0.5$ . Note that at the point of maximum wind the vertical and radial velocities are usually much smaller than the tangential velocity, so  $v^2 \approx V^2$ , where  $V$  is total air velocity.

Using the definitions of  $\mathcal{C}$  (8) and  $\mathcal{B}$  (10), Eq. (7) can be written as

$$\frac{1}{(1+\zeta)} \frac{T}{\mathcal{B}\mathcal{C}} \frac{\partial s^*}{\partial r} = -\frac{v^2}{r}. \quad (11)$$

This equation has a general validity. Its comparison with Eq. (4) reveals that the flow being supergradient ( $\mathcal{B} < 1$ ) and air temperature declining towards the storm center ( $\mathcal{C} < 1$ ) cause E-PI to underestimate  $v_m$  more than it does in the radially balanced isothermal case ( $\mathcal{B} = 1, \mathcal{C} = 1$ ). Conversely, for E-PI's Eq. (4) to be consistent with observations for a radially balanced ( $\mathcal{B} = 1$ ) or supergradient ( $\mathcal{B} \leq 1$ ) flow, the temperature at the point of maximum wind must increase towards the hurricane center ( $\mathcal{C} > 1$ ).

### 3.2 Hurricane Isabel 2003

When, as is the case in the stronger storms, the pressure gradient is sufficiently steep and the radial motion sufficiently rapid, the radial expansion of air is accompanied by a drop of temperature. In the well-studied Hurricane Isabel 2003 the surface air cooled by about 4 K while moving from the outer core (150-250 km) to the eyewall (40-50 km) (Montgomery et al., 2006, Fig. 4c). Over the same distance, the surface pressure fell by less than about 50 hPa (from less than 1013 hPa to 960 hPa) (Aberson et al., 2006, Fig. 4). (Air pressure at the outermost closed isobar  $\sim 465$  km from the center was 1013 hPa, hence at 150-250 km from the center it should have been smaller.) With  $\Delta p \approx -45$  hPa and  $\Delta T \approx -4$  K, at  $T = 297$  K and  $p \approx 10^3$  hPa, the horizontal temperature gradient at the surface  $\Delta T/\Delta p = 0.09$  K hPa $^{-1}$  approaches the dry adiabatic gradient  $\Gamma_d = \mu T/p = 0.1$  K hPa $^{-1}$  (see Fig. 1b).

At the top of the boundary layer the radial flow is weaker than it is on the surface, and the mean horizontal temperature gradient is smaller. At the level of maximum wind  $z_m = 1$  km in Hurricane Isabel 2003 the temperature difference between the eyewall and the outer core was  $\Delta T \approx -2$  K (Montgomery et al., 2006, Fig. 4c). Assuming that the pressure difference at this level is about 0.9 of its value at the surface,  $\Delta p \approx -0.9 \times 45$  hPa, we have  $\Delta T/\Delta p = 0.05$  K hPa $^{-1}$ . The mean horizontal temperature gradient between the outer core and the eyewall at the top of the boundary layer approaches the moist adiabatic gradient  $\Gamma = 0.04$  K hPa $^{-1}$  for  $T = 293$  K and  $p = 850$  hPa (Fig. 1b).

In the eye, the sunlight and the descending air motion work to elevate the air temperature above that at the eyewall and in the outer core. The air temperature in the eye rises towards the storm center and  $\partial T/\partial r < 0$ . For Hurricane Isabel 2003, with pressure and temperature differences at  $z_m = 1$  km between the eye and the eyewall  $\Delta p \approx -30$  hPa (Aberson et al., 2006, Fig. 4) and  $\Delta T = 3$  K (Montgomery et al., 2006, Fig. 4c), for  $p = 850$  hPa and  $T = 293$  K we have  $\Delta T/\Delta p = -0.1$  K hPa $^{-1} \approx -2.5\Gamma$  (Fig. 1b).

That the horizontal temperature gradient changes its sign somewhere in the eyewall suggests that  $\partial T/\partial r = 0$  at the point of maximum wind is a plausible assumption. However, the magnitudes of horizontal temperature gradients on both sides of the eyewall are large enough to significantly impact the maximum velocity estimates (Fig. 1b).

For example, if at the point of maximum wind the horizontal temperature gradient were close to  $\Gamma$  (as it was on average between the eyewall and the outer core in Hurricane Isabel 2003), then  $\mathcal{C} \rightarrow 0$  and  $\mathcal{BC}(1 + \zeta)\varepsilon \rightarrow 0$ . In this case E-PI would formally infinitely *underestimate*  $v_m^2$ . Physically, this limit corresponds to the situation when the moist adiabat is locally horizontal,  $\partial s^*/\partial r \rightarrow 0$ , such that the dependence between saturated moist entropy and maximum velocity vanishes, see in Eq. (11).

If, on the other hand, at the point of maximum wind the horizontal temperature gradient were equal to  $-2.5\Gamma$  (as it was on average between the eye and the eyewall in Hurricane Isabel 2003), then  $\mathcal{C} = 3.5$  and E-PI's Eq. (4) would *overestimate*  $v_m^2$  by  $\mathcal{BC}(1 + \zeta)\varepsilon = 1.4$ -fold for a balanced flow ( $\mathcal{B} = 1$ ). With  $\mathcal{B} = 0.8$  as discussed above, the overestimate reduces to 1.1 (about 10%).

For a known  $\mathcal{B}$ , the value of  $\mathcal{C}$  can be derived from the observed values of variables entering Eq. (11). The data for Hurricane Isabel 2003 suggest that at the point of maximum wind the air temperature increases towards the center  $\mathcal{C} > 1$ , but not enough to bring E-PI in agreement with observations: on September 12 and 14, E-PI underestimates  $v_m^2$  by about 50% and 30%, respectively (Table 1).

The closest agreement is observed on September 13, when  $\mathcal{C}$  is the largest (Fig. 1b). Given that the flow at this date was supergradient with  $\mathcal{B} \approx 0.8$  (Bell and Montgomery, 2008), this agreement does not indicate that the storm is in thermal wind balance (cf. Montgomery et al., 2006, p. 1345). Rather, it suggests that the large value of  $\mathcal{C} = 2.9$  nearly compensated the underestimate that would have otherwise resulted from  $\mathcal{B} < 1$ . The underestimate is greatest on September 12, when the local temperature gradient is closest to zero (Fig. 1b) and  $\mathcal{C}$  is close to unity (Table 1).

**Table 1.** Parameters of Eqs. (11) and E-PI's Eq. (4) estimated from observations for Hurricane Isabel 2003.

Date	$r_m$ , km	$T_o$ , °C	$\theta_e$ , K	$\partial\theta_e/\partial r$ , K km <sup>-1</sup>	$\tilde{v}_m$ , m s <sup>-1</sup>	$v_m$ , m s <sup>-1</sup>	$\varepsilon$	$(1 + \zeta)\varepsilon$	$(v_m/\tilde{v}_m)^2$	$\mathcal{C}$
12 September	25	-65	360	-0.5	80	54	0.29	0.43	0.46	1.3
13 September	45	-58	357	-0.6	76	74	0.27	0.40	0.96	2.9
14 September	50	-56	357	-0.35	74	61	0.26	0.39	0.68	2.1

Notes. Observed values of  $r_m$ ,  $T_o$ ,  $\tilde{v}_m$  and  $\partial\theta_e/\partial r$  are taken from, respectively, the first and the third columns of Table 2, and equivalent potential temperature  $\theta_e$  from Fig. 5, of Bell and Montgomery (2008). At the top of the boundary layer, temperature  $T_b = 293$  K (20°C) is assumed for all the three days based on Fig. 4c of Montgomery et al. (2006),  $\zeta = L\gamma_d^*/RT_b = 0.49$  for  $p_d = 850$  hPa and  $p_v^* = 23$  hPa. The values of  $v_m$  are E-PI estimates of maximum velocity obtained from Eq. (4), where  $\partial s^*/\partial r = (c_p/\theta_e)\partial\theta_e/\partial r$ ,  $c_p = 1$  kJ kg<sup>-1</sup> K<sup>-1</sup> (see Montgomery et al., 2006, Eq. A2). Factor  $(1 + \zeta)\varepsilon < 1$ , see Eq. (9), indicates by how much E-PI's Eqs. (6) and (4) would underestimate the squared maximum velocity under isothermal conditions in gradient wind balance;  $\mathcal{C}$  is estimated from Eq. (11) with  $\mathcal{B} = 0.8$ ,  $v = \tilde{v}_m$  and  $r = r_m$ .

## 4 Conclusions

In intense tropical cyclones, the radial air inflow significantly impacts the radial temperature gradient, which may change its sign in the vicinity of maximum wind. Thus, assuming that at the point of maximum wind the top of the boundary layer is horizontally isothermal appears justified. Here we showed that in this case one of the key relationships of E-PI, Eq. (4), underestimates the maximum wind speed by about twofold under common atmospheric conditions. This conclusion follows robustly from the definition of saturated moist entropy.

For E-PI's Eqs. (4) and (6) to conform to observations, the air temperature at the point of maximum wind must rise considerably towards the storm center. Such a pattern is possible if the storm is sufficiently intense to have a warm eye (where the higher temperature is ensured by the descending air motion and the incoming solar radiation under clear sky conditions). We considered this feature for Hurricane Isabel 2003 (Table 1). Our conclusion, that the warm eye can reduce the underestimate and drive the E-PI estimate up and closer to observations, runs somewhat counter to the suggestion of Bell and Montgomery (2008) that the extra heat from the eye may be the *cause* of E-PI underestimating the actual velocity. Without a warm eye (and hence without  $C > 1$ ), the E-PI's relationship at the top of the boundary layer would have underestimated the storm intensity even more significantly.

In the weaker cyclones without a well-defined eye, the existence of a pronounced temperature surplus at the storm center might be less likely. In such cyclones, E-PI at the top of the boundary layer should considerably underestimate maximum velocity (Fig. 1). E-PI in the weaker cyclones providing, instead, an upper limit on their intensities, indicates that a certain overcompensation occurs in the assumptions pertaining to the remaining two E-PI blocks, the boundary layer interior and the air-sea interface (Table 2, second and third rows).

In particular, Bryan and Rotunno (2009) showed that the E-PI key relationship for the boundary layer interior, that  $ds^*/dM$  is equal to the ratio  $\tau_s/\tau_M$  of the surface fluxes of entropy and momentum, overestimates the actual  $ds^*/dM$  ratio by up to 50%. This overestimate of  $ds^*/dM$  by  $\tau_s/\tau_M$  can partially compensate the underestimate of maximum velocity by E-PI's Eqs. (1) and (4) (see also Table 2, first row).

Another compensating overestimate results from E-PI's assumptions concerning the disequilibrium  $\Delta k = k_s^* - k = c_p \Delta T + L_v \Delta q$  at the air-sea interface at the radius of maximum wind (Table 2, second row). Since the local enthalpy difference  $\Delta k$  is unknown, E-PI limits it from above by assuming that the local difference in mixing ratios  $\Delta q$  is less than the water vapor deficit  $(1 - \mathcal{H}_a)q_{sa}^*$  in the ambient environment (Table 2, third row).

However, as Emanuel (1986) and Emanuel and Rotunno (2011) pointed out, in reality  $\Delta k$  tends to decline from the outer core towards the storm center. Indeed, if the radial inflow is sufficiently slow, as it is the case in the weaker storms, the surface air can remain in approximate thermal equilibrium with the oceanic surface. In his original evaluations of E-PI Emanuel (1986, p. 591) assumed  $\Delta T = 0$ . On the other hand, evaporation into the air parcels that are spiraling inward increases the relative humidity and diminishes  $\Delta q$ . In the result, in the weaker cyclones the actual  $\Delta k$  at the radius of maximum wind can be much lower than its ambient constraint  $(1 - \mathcal{H}_a)q_{sa}^*$ . This would overcompensate the underestimate of  $v_m$  at the top of the boundary

**Table 2.** Three logical blocks of E-PI.

Atmospheric region	Assumptions	Key relationship	References
Upper atmosphere and the top of boundary layer ( $z \geq z_b$ )	The air is in hydrostatic and gradient wind balance; surfaces of constant saturated moist entropy $s^*$ and angular momentum $M$ coincide	$-(T_1 - T_2) \frac{ds^*}{dM} = \frac{v_1}{r_1} - \frac{v_2}{r_2}$	Emanuel and Rotunno (2011, Eq. 11)
Boundary layer near the radius of maximum wind ( $0 < z \leq z_b$ )	Horizontal turbulent fluxes of $s^*$ and $M$ are negligible compared to vertical ones; surfaces of constant $s^*$ and $M$ are approximately vertical; turbulent fluxes of $s^*$ and $M$ vanish at $z = z_b$	$\frac{ds^*}{dM} = \frac{\tau_s}{\tau_M} = \frac{C_k k_s^* - k}{C_D T_s r v}$	Emanuel (1986, Eqs. 32, 33), Emanuel and Rotunno (2011, Eqs. 17, 19, 20)
Air-sea interface near the radius of maximum wind	The upper limit for the air-sea disequilibrium is set by the ambient relative humidity $\mathcal{H}_a$	$q_s^* - q \lesssim (1 - \mathcal{H}_a) q_{sa}^*$	(Emanuel, 1995, p. 3971), Emanuel (1989, Eq. 38)
Final E-PI estimate	For $\varepsilon \approx 0.3$ , $C_k/C_D \approx 1$ , $\mathcal{H}_a = 0.8$ and $T_s = 300$ K, $v_m \lesssim 60 \text{ m s}^{-1}$	$v_m^2 \lesssim \varepsilon \frac{C_k}{C_D} L_v (1 - \mathcal{H}_a) q_{sa}^*$	Emanuel (1989, Eq. 38 and Table 1)

Notes. In the first row,  $T_1, T_2$  and  $v_1, v_2$  are, respectively, air temperatures and tangential wind speeds at arbitrary points  $r_1$  and  $r_2$  on a streamline defined by the given value of  $ds^*/dM$ . In E-PI,  $r_1$  is chosen at the top of the boundary layer ( $z = z_b$ ) near the point  $r = r_m$  of maximum wind,  $r_2$  is chosen in the outflow in the upper atmosphere, such that either  $v_2 = 0$  or  $r_2 \rightarrow \infty$  and  $v_2/r_2 \rightarrow 0$ , see Eq. (1). In the second row,  $\tau_s$  and  $\tau_M$  are the surface fluxes of, respectively, entropy and angular momentum,  $C_k$  and  $C_D$  are exchange coefficients for enthalpy and momentum,  $r$  is local radius,  $k_s^*$  is saturated enthalpy at sea surface temperature  $T_s$ ,  $k_s^* - k = c_p(T_s - T) + L_v(q_s^* - q)$ , where  $c_p$  is the specific heat capacity of air at constant pressure,  $L_v$  is the latent heat of vaporization,  $q_s^*$  is the saturated mixing ratio at  $T_s$ ,  $v, k, q$  and  $T$  are the tangential wind, enthalpy, water vapor mixing ratio and air temperature at a reference height (usually about 10 m above the sea level). In the third row,  $\mathcal{H}_a$  and  $q_{sa}^*$  are the relative humidity and saturated mixing ratio at the surface temperature in the ambient environment outside the storm core.

layer by E-PI's Eq. (4) and explain why in many cases the E-PI final expression (Table 2, forth row) goes above the observed maximum velocities.

In the stronger storms like hurricanes, however, the air streams so quickly towards the center that it cools significantly compared to the isothermal oceanic surface it moves above. As discussed by Camp and Montgomery (2001) and Montgomery et al. (2006), this cooling tends to offset the increase in relative humidity, such that the mixing ratio  $q$  does not considerably grow, and  $\Delta q$  does not diminish significantly, towards the center. In this case the E-PI's assumption,  $\Delta q \approx (1 - \mathcal{H}_a) q_{sa}^*$ , becomes valid. No overcompensation occurs in the third block of E-PI. As a result, in the strongest storms the underestimate stemming from the first block of E-PI becomes explicit.

On the other hand, that the final E-PI expression (Table 2, forth row) produces a plausible if not 100% robust upper limit on maximum intensity (despite deriving from assumptions that systematically underestimate and overestimate intensities), can be explained by the fact that the quantitative parameters in the final expression for kinetic energy incidentally combine into the partial pressure of water vapor (see Eqs. (A.12)–(A.14) in the Appendix). Partial pressure of water vapor has been suggested



to be the key parameter of hurricane dynamics (Makarieva et al., 2014). Its exponential temperature dependence would explain that of E-PI.

The alternative relationship between the radial gradient of saturated moist entropy and maximum velocity, Eq. (11), reveals the profound influence of the radial temperature gradient on storm intensity. While until now the radial temperature gradient at the top of the boundary layer has not received much attention in the assessments of E-PI's validity (e.g., Montgomery et al., 2006; Bryan and Rotunno, 2009; Emanuel and Rotunno, 2011), our results highlight the need to pay more attention to the radial change of air temperature in further studies.

### Appendix: Details of derivations

Using the definition of angular momentum  $M$  (2), we obtain

$$\frac{M}{r^2} \frac{\partial M}{\partial r} = \left( \frac{v}{r} + \frac{f}{2} \right) \left( v + fr + r \frac{\partial v}{\partial r} \right) = \frac{v^2}{r} + fv + v \frac{\partial v}{\partial r} + \frac{f}{2} \left( v + fr + r \frac{\partial v}{\partial r} \right) = \alpha \frac{\partial p}{\partial r} \left( 1 + \frac{fr}{2v} \right). \quad (\text{A.1})$$

The last equality assumes the condition  $\partial v / \partial r = 0$  (the point of maximum wind) and the gradient wind balance (5).

Saturated moist entropy is defined as (see Pauluis, 2011, Eq. A4)

$$s^* = (c_{pd} + q_t c_l) \ln \frac{T}{T_0} - \frac{R}{M_d} \ln \frac{p_d}{p_0} + q^* \frac{L_v}{T}. \quad (\text{A.2})$$

Here,  $L_v = L_{v0} + (c_{pv} - c_l)(T - T_0)$  is the latent heat of vaporization ( $\text{J kg}^{-1}$ );  $q^* = \rho_v^* / \rho_d$ ,  $q_l = \rho_l / \rho_d$ , and  $q_t = q^* + q_l$  are the mixing ratio for saturated water vapor, liquid water, and total water, respectively;  $\rho_d$ ,  $\rho_v^*$ , and  $\rho_l$  are the density of dry air, saturated water vapor and liquid water, respectively;  $c_{pd}$  and  $c_{pv}$  are the specific heat capacities of dry air and water vapor at constant pressure;  $c_l$  is the specific heat capacity of liquid water;  $R = 8.3 \text{ J mol}^{-1} \text{ K}^{-1}$  is the universal gas constant;  $M_d$  is the molar mass of dry air;  $p_d$  is the partial pressure of dry air;  $T$  is the temperature;  $p_0$  and  $T_0$  are reference air pressure and temperature.

From Eq. (A.2) we have

$$T ds^* = (c_{pd} + q_t c_l) dT - \frac{RT}{M_d} \frac{dp_d}{p_d} + L_v dq^* + q^* dL_v - q^* L_v \frac{dT}{T} = \left( c_p - \frac{q^* L_v}{T} \right) dT - \frac{RT}{M_d} \frac{dp_d}{p_d} + L_v dq^*, \quad (\text{A.3})$$

where  $c_p \equiv c_{pd} + q^* c_{pv} + q_l c_l$  and  $dL_v = (c_{pv} - c_l) dT$ . Equation (A.3) assumes  $q_t = \text{const}$  (reversible adiabat).

The ideal gas law for the partial pressure  $p_v$  of water vapor is

$$p_v = N_v RT, \quad N_v = \frac{\rho_v}{M_v}, \quad (\text{A.4})$$

where  $M_v$  and  $\rho_v$  are the molar mass and density of water vapor. Using Eq. (A.4) with  $p_v = p_v^*$  in the definition of  $q^*$

$$q^* \equiv \frac{\rho_v^*}{\rho_d} = \frac{M_v p_v^*}{M_d p_d} \equiv \frac{M_v}{M_d} \gamma_d^*, \quad \gamma_d^* \equiv \frac{p_v^*}{p_d}, \quad (\text{A.5})$$

and applying the Clausius-Clapeyron law

$$\frac{dp_v^*}{p_v^*} = \frac{L}{RT} \frac{dT}{T}, \quad L \equiv L_v M_v, \quad (\text{A.6})$$

we obtain for the last term in Eq. (A.3)

$$L_v dq^* = L_v \frac{M_v}{M_d} \left( \frac{dp_v^*}{p_d} - \frac{p_v^* dp_d}{p_d p_d} \right) = L_v \frac{M_v}{M_d} \left( \frac{p_v^* dp_v^*}{p_d p_v^*} - \frac{p_v^* dp_d}{p_d p_d} \right) = L_v q^* \left( \frac{L}{RT} \frac{dT}{T} - \frac{dp_d}{p_d} \right). \quad (\text{A.7})$$

Using the Clausius-Clapeyron law (A.6), the ideal gas law  $p_d = N_d RT$ , where  $N_d = \rho_d / M_d$ , and noting that  $p = p_v^* + p_d$ , we obtain for the last but one term in Eq. (A.3)

$$\frac{RT}{M_d} \frac{dp_d}{p_d} = \frac{RT}{M_d} \left( \frac{dp}{p_d} - \frac{dp_v^*}{p_d} \right) = \frac{dp}{M_d N_d} - \frac{RT p_v^* dp_v^*}{M_d p_d p_v^*} = \frac{dp}{\rho_d} - L_v \frac{M_v p_v^*}{M_d p_d} \frac{dT}{T} = \frac{dp}{\rho_d} - q^* L_v \frac{dT}{T}. \quad (\text{A.8})$$

Putting Eqs. (A.7) and (A.8) into Eq. (A.3) yields

$$T ds^* = \left( c_p + \frac{L_v q^*}{T} \frac{L(1 + \gamma_d^*)}{RT} \right) dT - \left( 1 + \frac{L \gamma_d^*}{RT} \right) \frac{dp}{\rho_d} = -(1 + \zeta) \alpha_d dp \left( 1 - \frac{1}{\Gamma} \frac{dT}{dp} \right). \quad (\text{A.9})$$

Here

$$\Gamma \equiv \frac{\alpha_d}{c_p} \frac{1 + \zeta}{1 + \mu \zeta (\xi + \zeta)}, \quad \xi \equiv \frac{L}{RT}, \quad \zeta \equiv \xi \gamma_d^*, \quad \mu \equiv \frac{R}{C_p} = \frac{2}{7}, \quad (\text{A.10})$$

where  $\alpha_d \equiv 1/\rho_d$  is the volume per unit mass of dry air and  $C_p = c_p M_d$  is the molar heat capacity of air at constant pressure.

Approximating air molar mass by molar mass  $M_d$  of dry air and  $c_p$  by  $c_{pd}$ , we can conveniently express  $\Gamma$  as

$$\Gamma \approx \frac{T}{p} \frac{\mu(1 + \zeta)}{1 + \mu \zeta (\xi + \zeta)} \approx \frac{T}{p} \frac{\mu(1 + \xi \gamma_d^*)}{1 + \mu \xi^2 \gamma_d^*}. \quad (\text{A.11})$$

Using Eq. (A.5) and  $q \equiv \mathcal{H} q^*$ , where  $\mathcal{H} \equiv p_v/p_v^*$  is relative humidity, the final E-PI expression for  $v_m$  (Table 2, forth row) can be re-written as follows:

$$v_m^2 \sim \left( \frac{1}{2} \varepsilon \frac{C_k}{C_D} \frac{L}{RT_s} \frac{1 - \mathcal{H}_a}{\mathcal{H}_a} \right) \frac{2 p_{vsa}}{\rho_{sa}}. \quad (\text{A.12})$$

Here  $p_{vsa} = \mathcal{H}_a p_{vsa}^*$  is the actual partial pressure of water vapor in surface air in the ambient environment,  $p_{vsa}^*$  is the partial pressure of saturated water vapor at sea surface temperature in the ambient environment,  $\rho_{sa}$  is ambient air density at the surface. Using typical tropical values  $T_s = 300$  K,  $\mathcal{H}_a = 0.8$ ,  $\rho_{sa} \approx 1.2$  kg m<sup>-3</sup>,  $\varepsilon = 0.32$  (Table 1 of Emanuel, 1989) and  $C_k/C_D = 1$ , we have  $p_{vs} = 28$  hPa and  $v_m \approx 60$  m s<sup>-1</sup> in agreement with Table 1 of Emanuel (1989).

The coefficient in parentheses in Eq. (A.12) for the same typical parameters is close to unity and depends only weakly on air temperature:

$$\frac{1}{2} \varepsilon \frac{C_k}{C_D} \frac{L}{RT_s} \frac{1 - \mathcal{H}_a}{\mathcal{H}_a} \approx 1. \quad (\text{A.13})$$

This means that numerically the scaling of maximum velocity in E-PI practically coincides with the scaling

$$\rho_{sa} \frac{v_m^2}{2} = p_{vsa} \quad (\text{A.14})$$

proposed within the concept of condensation-induced atmospheric dynamics (for a more detailed discussion see Makarieva et al., 2019, Section 5). Introducing the dissipative heating leads to additional factor  $1/(1 - \varepsilon) \sim 1$  in Eq. (A.13) and the final E-PI expression for  $v_m^2$  (Table 2, forth row) (for a discussion, we refer to Makarieva et al., 2010; Bister et al., 2011; Kieu, 2015; Bejan, 2019; Makarieva et al., 2020; Emanuel and Rousseau-Rizzi, 2020)<sup>1</sup>.

---

<sup>1</sup>Emanuel and Rousseau-Rizzi (2020) equate quantities of different dimensions (see their Eq. (6) and related). This error is due to an incorrect transition from volume to surface fluxes (Makariev et al., 2020).

## References

- Aberson, S. D., Montgomery, M. T., Bell, M., and Black, M.: Hurricane Isabel (2003): New insights into the physics of intense storms. Part II: Extreme localized wind, *Bull. Amer. Meteor. Soc.*, 87, 1349–1354, doi:10.1175/BAMS-87-10-1349, 2006.
- Bejan, A.: Thermodynamics of heating, *Proc. Roy. Soc.*, 475A, 20180 820, doi:10.1098/rspa.2018.0820, 2019.
- Bell, M. M. and Montgomery, M. T.: Observed structure, evolution, and potential intensity of category 5 Hurricane Isabel (2003) from 12 to 14 September, *Mon. Wea. Rev.*, 136, 2023–2046, doi:10.1175/2007MWR1858.1, 2008.
- Bister, M., Renno, N., Pauluis, O., and Emanuel, K.: Comment on Makarieva *et al.* ‘A critique of some modern applications of the Carnot heat engine concept: the dissipative heat engine cannot exist’, *Proc. Roy. Soc.*, 467A, 1–6, doi:10.1098/rspa.2010.0087, 2011.
- Bryan, G. H. and Rotunno, R.: Evaluation of an analytical model for the maximum intensity of tropical cyclones, *J. Atmos. Sci.*, 66, 3042–3060, doi:10.1175/2009JAS3038.1, 2009.
- Camp, J. P. and Montgomery, M. T.: Hurricane maximum intensity: Past and present, *Mon. Wea. Rev.*, 129, 1704–1717, doi:10.1175/1520-0493(2001)129<1704:HMIPAP>2.0.CO;2, 2001.
- DeMaria, M. and Kaplan, J.: Sea surface temperature and the maximum intensity of Atlantic tropical cyclones, *J. Climate*, 7, 1324–1334, doi:10.1175/1520-0442(1994)007<1324:SSTATM>2.0.CO;2, 1994.
- Emanuel, K.: The relevance of theory for contemporary research in atmospheres, oceans, and climate, *AGU Advances*, 1, e2019AV000 129, doi:10.1029/2019AV000129, 2020.
- Emanuel, K. and Rotunno, R.: Self-Stratification of Tropical Cyclone Outflow. Part I: Implications for Storm Structure, *J. Atmos. Sci.*, 68, 2236–2249, doi:10.1175/JAS-D-10-05024.1, 2011.
- Emanuel, K. and Rousseau-Rizzi, R.: Reply to “Comments on ‘An evaluation of hurricane superintensity in axisymmetric numerical models’”, *J. Atmos. Sci.*, 77, 3977–3980, doi:10.1175/JAS-D-20-0199.1, 2020.
- Emanuel, K. A.: An air-sea interaction theory for tropical cyclones. Part I: Steady-state maintenance, *J. Atmos. Sci.*, 43, 585–604, doi:10.1175/1520-0469(1986)043<0585:AASITF>2.0.CO;2, 1986.
- Emanuel, K. A.: The finite-amplitude nature of tropical cyclogenesis, *J. Atmos. Sci.*, 46, 3431–3456, doi:10.1175/1520-0469(1989)046<3431:TFANOT>2.0.CO;2, 1989.
- Emanuel, K. A.: Sensitivity of tropical cyclones to surface exchange coefficients and a revised steady-state model incorporating eye dynamics, *J. Atmos. Sci.*, 52, 3969–3976, doi:10.1175/1520-0469(1995)052<3969:SOTCTS>2.0.CO;2, 1995.
- Frank, W. M.: The structure and energetics of the tropical cyclone I. Storm structure, *Mon. Wea. Rev.*, 105, 1119–1135, doi:10.1175/1520-0493(1977)105<1119:TSAEOT>2.0.CO;2, 1977.
- Garner, S.: The relationship between hurricane potential intensity and CAPE, *J. Atmos. Sci.*, 72, 141–163, doi:10.1175/JAS-D-14-0008.1, 2015.
- Kieu, C.: Revisiting dissipative heating in tropical cyclone maximum potential intensity, *Quart. J. Roy. Meteor. Soc.*, 141, 2497–2504, doi:10.1002/qj.2534, 2015.
- Kieu, C. Q. and Moon, Z.: Hurricane intensity predictability, *Bull. Amer. Meteor. Soc.*, 97, 1847–1857, doi:10.1175/BAMS-D-15-00168.1, 2016.
- Kowaleski, A. M. and Evans, J. L.: A reformulation of tropical cyclone potential intensity theory incorporating energy production along a radial trajectory, *Mon. Wea. Rev.*, 144, 3569–3578, doi:10.1175/MWR-D-15-0383.1, 2016.

- Li, Y., Wang, Y., Lin, Y., and Fei, R.: Dependence of superintensity of tropical cyclones on SST in axisymmetric numerical simulations, *Mon. Wea. Rev.*, 148, 4767–4781, doi:10.1175/MWR-D-20-0141.1, 2020.
- Makarieva, A. M., Gorshkov, V. G., Li, B.-L., and Nobre, A. D.: A critique of some modern applications of the Carnot heat engine concept: the dissipative heat engine cannot exist, *Proc. Roy. Soc.*, 466A, 1893–1902, doi:10.1098/rspa.2009.0581, 2010.
- Makarieva, A. M., Gorshkov, V. G., and Nefiodov, A. V.: Condensational power of air circulation in the presence of a horizontal temperature gradient, *Phys. Lett. A*, 378, 294–298, doi:10.1016/j.physleta.2013.11.019, 2014.
- Makarieva, A. M., Gorshkov, V. G., Nefiodov, A. V., Chikunov, A. V., Sheil, D., Nobre, A. D., Nobre, P., and Li, B.-L.: Hurricane’s maximum potential intensity and surface heat fluxes, arXiv, <https://arxiv.org/abs/1810.12451v2>, 2019.
- Makarieva, A. M., Nefiodov, A. V., Sheil, D., Nobre, A. D., Chikunov, A. V., Plunien, G., and Li, B.-L.: Comments on “An evaluation of hurricane superintensity in axisymmetric numerical models”, *J. Atmos. Sci.*, 77, 3971–3975, doi:10.1175/JAS-D-20-0156.1, 2020.
- Montgomery, M. T., Bell, M. M., Aberson, S. D., and Black, M. L.: Hurricane Isabel (2003): New insights into the physics of intense storms. Part I: Mean vortex structure and maximum intensity estimates, *Bull. Amer. Meteor. Soc.*, 87, 1335–1347, doi:10.1175/BAMS-87-10-1335, 2006.
- Pauluis, O.: Water vapor and mechanical work: A comparison of Carnot and steam cycles, *J. Atmos. Sci.*, 68, 91–102, doi:10.1175/2010JAS3530.1, 2011.
- Persing, J. and Montgomery, M. T.: Hurricane superintensity, *J. Atmos. Sci.*, 60, 2349–2371, doi:10.1175/1520-0469(2003)060<2349:HS>2.0.CO;2, 2003.
- Rousseau-Rizzi, R. and Emanuel, K.: An evaluation of hurricane superintensity in axisymmetric numerical models, *J. Atmos. Sci.*, 76, 1697–1708, doi:10.1175/JAS-D-18-0238.1, 2019.
- Tao, D., Bell, M., Rotunno, R., and van Leeuwen, P. J.: Why do the maximum intensities in modeled tropical cyclones vary under the same environmental conditions?, *Geophys. Res. Lett.*, 47, e2019GL085980, doi:10.1029/2019GL085980, 2020.